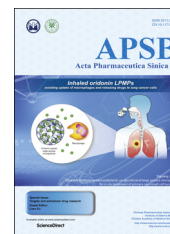




Chinese Pharmaceutical Association
Institute of Materia Medica, Chinese Academy of Medical Sciences

Acta Pharmaceutica Sinica B

www.elsevier.com/locate/apsb
www.sciencedirect.com



ORIGINAL ARTICLE

C0818, a novel curcumin derivative, interacts with Hsp90 and inhibits Hsp90 ATPase activity



Yingjuan Fan^{a,b}, Yang Liu^{a,b}, Lianru Zhang^c, Fang Cai^{a,b},
Liping Zhu^{a,b}, Jianhua Xu^{a,b,*}

^aSchool of Pharmacy, Fujian Medical University, Fuzhou 350108, China

^bFujian Provincial Key Laboratory of Natural Medicine Pharmacology, Fuzhou 350108, China

^cSchool of Life Science, Xiameng University, Xiamen 361005, China

Received 30 January 2016; received in revised form 16 April 2016; accepted 6 May 2016

KEY WORDS

Curcumin derivative;
Hsp90;
ATPase activity;
Fluorescence spectrometry;
Interaction

Abstract The aims of the present study were to estimate the affinity between 3,5-(*E*)-bis(3-methoxy-4-hydroxybenzal)-4-piperidinone hydrochloride (C0818) and heat shock protein 90 (Hsp90) and to investigate the inhibitory effects of this compound on Hsp90 ATPase activity. Fluorescence spectroscopy was used to examine the affinity between varying concentrations of C0818 and Hsp90, N-Hsp90, M-Hsp90 and C-Hsp90. Fluorescence intensities were recorded in the range of 290–510 nm at 293, 303 and 310 K, respectively. A colorimetric assay for inorganic phosphate (based on the formation of a phosphomolybdate complex and the subsequent reaction with malachite green) were used to examine the inhibitory effects of C0818 on Hsp90 ATPase activity. The equilibrium dissociation constant K_D value of C0818 was found to be $23.412 \pm 0.943 \mu\text{mol/L}$. The interaction between C0818 and Hsp90 was driven mainly by electrostatic interactions. C0818 showed the strongest affinity with C-Hsp90. These results conclusively demonstrate the inhibitory activity of C0818 on the activity of Hsp90 ATPase.

© 2017 Chinese Pharmaceutical Association and Institute of Materia Medica, Chinese Academy of Medical Sciences. Production and hosting by Elsevier B.V. This is an open access article under the CC BY-NC-ND license (<http://creativecommons.org/licenses/by-nc-nd/4.0/>).

*Corresponding author at: School of Pharmacy, Fujian Medical University, Fuzhou 350108, China. Tel.: +86 59122862029.

E-mail address: xjh@mail.fjmu.edu.cn (Jianhua Xu).

Peer review under responsibility of Institute of Materia Medica, Chinese Academy of Medical Sciences and Chinese Pharmaceutical Association.

1. Introduction

Heat shock protein 90 (Hsp90) is an ATP-dependent cellular chaperone responsible for maintaining the stability and activity of a number of client proteins involved in cell signaling, proliferation and survival^{1,2}. Recent studies have shown that Hsp90 is a key protein for oncogenesis and malignancy, and an emerging target for cancer therapeutics^{3–6}. Hsp90 inhibitors can simultaneously inhibit multiple signaling pathways that cancer cells depend on for their growth and proliferation. Since Hsp90 inhibitors have significant potential as antitumor agents, the discovery of Hsp90 inhibitors with new chemical scaffolds is relevant to advances in cancer chemotherapy.

The chaperoning of most Hsp90 client proteins is regulated by a dynamic cycle driven by ATP binding to Hsp90 and subsequent hydrolysis of the protein⁷. The intrinsic ATPase activity of Hsp90 is essential to this activity. Inhibition of the ATPase activity of Hsp90 leads to antitumor activity *in vitro* and *in vivo*^{8,9}.

Curcumin is an active ingredient of the plant turmeric (*Curcuma longa*). In our previous work¹⁰, we found that curcumin is a lead compound in the search for new kinds of Hsp90 inhibitors. We thus synthesized a series of derivatives, some of which showed lead-like properties and were found to be more active than curcumin in Hsp90 inhibition and antitumor action^{11,12}. In the present paper, we have investigated a novel curcumin derivative, 3,5-(*E*)-bis(3-methoxy-4-hydroxybenzyl)-4-piperidinone hydrochloride (C0818), for its interaction with Hsp90 and its inhibitory effect on the activity of Hsp90 ATPase.

2. Materials and methods

2.1. Materials and reagents

Bacterial strains and plasmids were provided by Prof. Lianru Zhang from School of Life Science, Xiamen University, China. C0818 was designed and synthesized by our laboratory (Fig. 1). Ni²⁺-nitrilotriacetic acid (NTA) agarose was purchased from General Electric (Little Chalfont, Buckinghamshire, England). ATP was purchased from Sigma-Aldrich (St. Louis, MO, USA). Geldanamycin (GA) was purchased from Shanghai Sangon Biological Engineering (Lot. No. XP0806132012J, Shanghai, China). A stock solution of Hsp90, which was expressed and purified by our laboratory, was prepared in a 10 mmol/L PBS buffer with a pH 7.4, and the applied concentration was fixed at 5.0 μmol/L. C0818 was dissolved in 5% DMSO for fluorescence measurements. The water used in the experiments was thrice-distilled using a Milli-Q Biocel system (Millipore, Bedford, MA, USA). All other reagents were of analytical reagent grade.

2.2. Cloning, expression, and purification Hsp90

Yeast Hsp90 recombinant plasmid (Hsp90-PET-28a) was used to transform the target constructs of Hsp90 to express in the strain

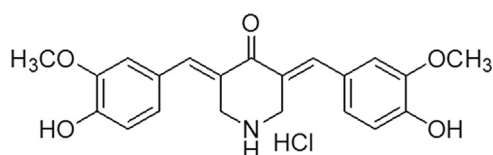


Figure 1 Chemical structure of C0818.

Escherichia coli BL21(DE3). The monoclonal cell was picked and cultured in lysogeny broth (LB) at 37 °C. Various constructs of Hsp90, including histidine (his)-tagged yeast full-length Hsp90 (1–732, 90 kDa), the N-terminal domain of Hsp90 (N-Hsp90, 1–236, 25 kDa), the middle domain of Hsp90 (M-Hsp90, 272–617, 40 kDa) and the C-terminal domain of Hsp90 (C-Hsp90, 629–732, 15 kDa), were induced by IPTG (isopropyl β-D-1-thiogalactopyranoside) and expressed in bacterial strains and purified by Ni²⁺-NTA (nitrilotriacetic acid) and gel filtration¹³.

2.3. Fluorescent measurements

Samples were excited at 280 nm and fluorescence intensities were recorded in the range of 290–500 nm at 293, 303 and 310 K, respectively, using a Cary Eclipse (Varian, Palo Alto, CA, USA). Fluorometric titration experiments were performed in 2.0 mL of 5.0 μmol/L Hsp90 solution (10 mmol/L PBS buffer, pH 7.6) with successive additions of C0818 solution (in 0.2% DMSO) from 5.0 to 50 μmol/L. All tests were performed in triplicate¹⁴.

2.4. Hsp90 ATPase activity assay

The reaction was performed in 100 μL of assay buffer (6 mmol/L MgCl₂, 20 mmol/L KCl and 100 mmol/L Tris-HCl, pH 7.4) containing 0.4 μmol/L Hsp90, 1 mmol/L ATP and different concentrations of C0818 or GA or vehicle (DMSO) and incubated at 310 K for 3 h. At the end of the incubation, the ATPase activity of Hsp90 were assessed by malachite green reagent (0.0812% w/v malachite green, 2.32% w/v polyvinyl alcohol and 5.72% w/v ammonium molybdate in 6 mol/L HCl, and argon water mixed in a ratio of 2:1:1:2, v/v/v/v). Cultures were analyzed in triplicate at an absorbance of 620 nm¹³. The kinetic analysis of the Hsp90 ATPase activity was carried out using a nonlinear regression fit of the experimental points to the Michaelis–Menten equation. To obtain K_m and V values, the Eadie–Hofstee linear transformation (V against $V/[s]$) was used, with the slope = $-K_m$ and the intercept on the x axis = V/K_m ¹³.

2.5. Statistical analysis

All data were analyzed with two-sided unpaired *t*-test in the GraphPad software package for Windows (Prism version 5.0) and Origin8.5 software. Values are expressed as means of triplicate or duplicate experiments.

3. Results

3.1. The interaction between C0818 and Hsp90

3.1.1. C0818 quenched the intrinsic fluorescence of Hsp90

The binding of C0818 to Hsp90 was characterized by fluorescence quenching. At excitation wavelength of 280 nm, the interaction was examined with fluorescence spectrum from 290 to 510 nm. His-tagged Hsp90 displayed maximal fluorescence at 334 nm. When Hsp90 was incubated with increasing concentrations of C0818, the fluorescence intensity gradually decreased with a slight blue shift of λ_{em} (Fig. 2A).

The dissociation constants (K_D) is calculated by the equation:

$$\Delta F = F_0 - F = F_{max} [Q] / K_D + [Q] \quad (1)$$

where F_0 is the steady-state fluorescence intensity of Hsp90, F is the fluorescence intensity of Hsp90 in presence of C0818 at

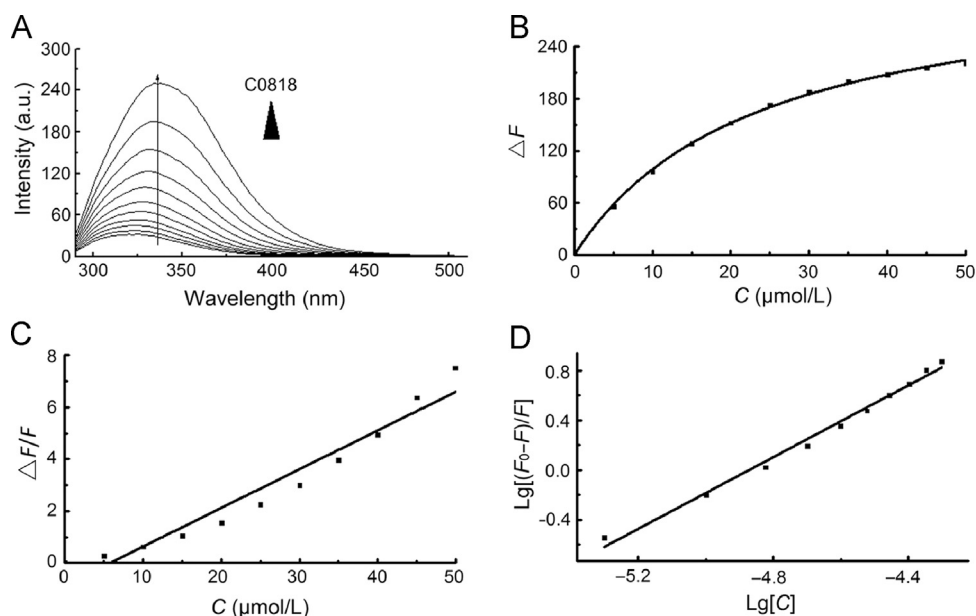


Figure 2 C0818 physically binds to Hsp90. (A) Quenching effect of C0818 (0–50 $\mu\text{mol/L}$) on Hsp90 endogenous fluorescent in a concentration-dependent manner. The maximal fluorescence displayed at 334 nm. (B) The change trend of Hsp90 fluorescence intensity with C0818 concentration. (C) Stern–Volmer plot for the binding of C0818 with Hsp90. (D) Lineweaver–Burk plot for the binding of C0818 with Hsp90.

Table 1 Dissociation constant K_D values of C0818 and geldanamycin (GA).

Compound	F_{\max}	K_D ($\mu\text{mol/L}$)	R^2
GA	546.16 ± 7.92	24.39 ± 0.79	0.999
C0818	329.93 ± 5.79	23.41 ± 0.94	0.999

different concentrations, and $[Q]$ is the concentration of C0818. The titration curves for Hsp90 yields estimated dissociation constants (K_D) of C0818 for Hsp90, which is of $23.41 \pm 0.94 \mu\text{mol/L}$ (Fig. 2B), indicating that C0818 quenched the intrinsic fluorescence of Hsp90 and that there was a binding interaction between them¹⁵ (Table 1).

3.1.2. Quenching constant and quenching rate constant

The quenching process can be analyzed by Stern–Volmer equation:

$$F_0/F = 1 + K_{sv}[Q] = 1 + K_q\tau_0[Q] \quad (2)$$

where F_0 , F and $[Q]$ means the same as in Eq. (1), K_{sv} is the Stern–Volmer quenching constant in static quenching, K_q is the quenching rate constant, and τ_0 is endogenous fluorescence lifetime value of biological macromolecules¹⁶, which generally is 10^{-8} s. K_{sv} and K_q were obtained from the slope of F_0/F plotted against $[Q]$ (Fig. 2C) and the results are listed in Table 2.

The maximum dynamic collisional quenching constant of all kinds of quenching agent with biopolymers is 2.0×10^{10} L/mol/s, the quenching rate constant K_q of C0818 was greater than 2.0×10^{10} L/mol/s, indicating that the quenching effect of C0818 on intrinsic fluorescence of Hsp90 is not due to molecules collision in dynamic quenching, but due to the formation of complex in static quenching¹⁷.

3.1.3. Number of binding sites and constant

Static quenching complies with the Lineweaver–Burk equation¹⁸:

$$\text{Lg } F_0 - F/F = \text{Lg } K + n \text{Lg}[Q] \quad (3)$$

where F_0 , F and $[Q]$ means the same as in Eq. (1), K_A is the apparent binding constant, and n is the binding site. K_A and n were obtained from the intercept and slope of $\text{lg} F_0 - F/F$ plotted against $\text{lg}[Q]$ (Fig. 2D), respectively, and the results are listed in Table 3.

Table 3 The binding constant K_A and the binding number n of C0818 and GA.

Compound	K_A (L/mol)	n	R^2
GA	2.88×10^5	1.14 ± 0.04	0.986
C0818	1.04×10^7	1.44 ± 0.05	0.989

Table 2 The Stern–Volmer quenching constant K_{sv} and bimolecular quenching constant K_q of C0818 and GA.

Compound	K_q (L/mol/s)	K_{sv} (L/mol)	R^2
GA	$(7.67 \pm 0.44) \times 10^{12}$	$(7.67 \pm 0.44) \times 10^4$	0.968
C0818	$(1.49 \pm 0.12) \times 10^{13}$	$(1.49 \pm 0.12) \times 10^5$	0.943

3.1.4. Thermodynamic parameters

Over the temperature ranges examined and when the thermodynamic enthalpy change (ΔH^θ) did not vary significantly, van't Hoff's equation was used to obtain the values of ΔH^θ and entropy change (ΔS^θ):

$$\ln K_{D1}/K_{D2} = \Delta H^\theta (1/T_1 - 1/T_2)/R \quad (4)$$

$$\Delta G^\theta = \Delta H^\theta - T\Delta S^\theta = RT \ln K_D \quad (5)$$

where R is the thermodynamic gas constant and the value is 8.314 J/mol/K, T is thermodynamic temperature, K_D is corresponding dissociation constants at different temperatures, ΔG^θ is Gibbs free energy change. Fluorescence intensities were recorded in the range of 290–510 nm at 293, 303 and 310 K, respectively (Fig. 3).

The thermodynamic enthalpy change (ΔH^θ), entropy change (ΔS^θ) and free energy change (ΔG^θ) of C0818–Hsp90 binding were also calculated from the fluorescent spectrum, the results are listed in Table 4. The negative enthalpy change and positive entropy change suggest that electrostatic interaction predominated in stabilizing the C0818–Hsp90 complex¹⁹.

In order to further determine the interaction type between C0818 and Hsp90, a synchronous fluorescence method was used to study the impact of C0818 on Hsp90 conformation.

3.1.5. Impact of C0818 on Hsp90 conformation

Tyrosine (Tyr) and tryptophan (Trp) are the main source of protein fluorescence. When the D-value ($\Delta\lambda$) between excitation and emission wavelengths was stabilized at 15 or 60 nm, the synchronous fluorescence provided the characteristic information of Tyr or Trp residues.

When $\Delta\lambda$ was 15 or 60 nm, increasing concentrations of C0818 led to a dramatic decrease in fluorescence intensity, but the fluorescence peak position of Tyr or Trp residues remained the same (Fig. 4), indicating that the microenvironment of Tyr or Trp residues did not change after binding, and that the hydrophobic microenvironment did not obviously decrease. These results imply that the conformation of Tyr or Trp of Hsp90 did not change.

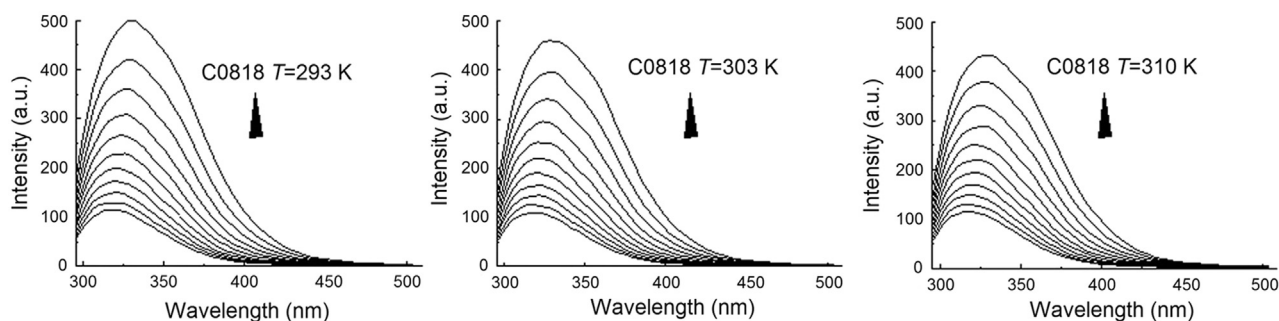


Figure 3 Quenching effect of C0818 (0–50 $\mu\text{mol/L}$) on Hsp90 endogenous fluorescent at different temperatures (293, 303 and 310 K).

Table 4 Dissociation constant K_D and thermodynamic parameters of C0818 and GA at different temperatures.

Compound	T (K)	K_D ($\mu\text{mol/L}$)	R^2	ΔG^θ (kJ/mol)	ΔH^θ (kJ/mol)	ΔS^θ (J/mol/K)
GA	293	18.63 ± 0.79	0.999	-26.53 ± 0.11	-11.20 ± 2.42	52.32 ± 8.00
	303	22.42 ± 0.65	0.999	-26.97 ± 0.07		
	310	24.39 ± 0.80	0.999	-27.37 ± 0.08		
C0818	293	39.13 ± 0.91	0.999	-24.72 ± 0.06	-12.96 ± 0.74	40.27 ± 2.45
	303	46.44 ± 1.72	0.999	-25.13 ± 0.09		
	310	53.44 ± 2.28	0.998	-25.35 ± 0.11		

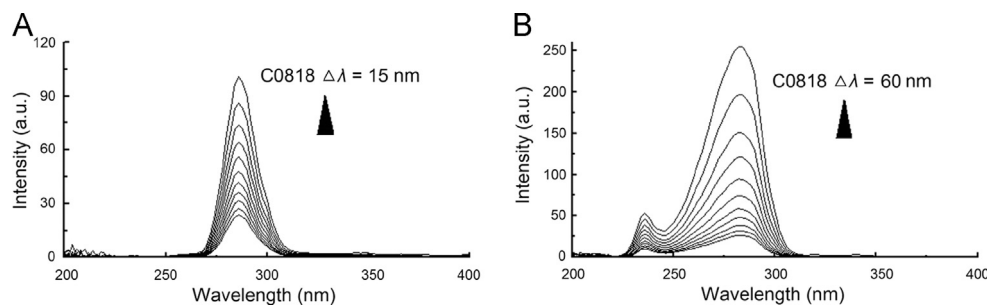


Figure 4 Synchronous fluorescence spectra of C0818 (0–50 $\mu\text{mol/L}$) with Hsp90. (A) $\Delta\lambda = 15$ nm; (B) $\Delta\lambda = 60$ nm.

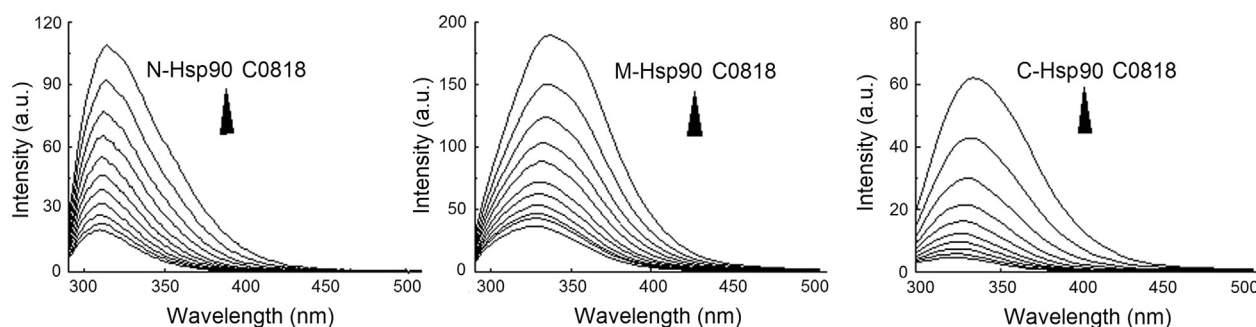


Figure 5 Quenching effect of C0818 (0–50 $\mu\text{mol/L}$) on endogenous fluorescent of N-Hsp90, M-Hsp90 and C-Hsp90.

Table 5 Dissociation constant K_D of C0818 and GA.

Interaction	F_{max}	K_D ($\mu\text{mol/L}$)	R^2
N-Hsp90–GA	221.22 ± 4.91	5.84 ± 0.61	0.991
M-Hsp90–GA	158.20 ± 1.68	42.13 ± 0.80	0.999
C-Hsp90–GA	67.91 ± 0.63	36.72 ± 0.64	0.999
N-Hsp90–C0818	159.48 ± 3.15	38.15 ± 1.40	0.999
M-Hsp90–C0818	232.46 ± 3.46	24.52 ± 0.82	0.999
C-Hsp90–C0818	76.51 ± 1.35	13.51 ± 0.68	0.998

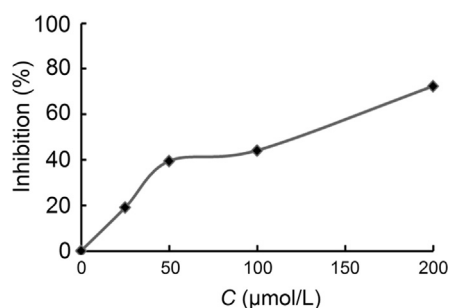


Figure 6 The inhibition rate of Hsp90 ATPase activity under different concentrations of C0818 (0–200 $\mu\text{mol/L}$).

3.1.6. The domain of Hsp90 binding C0818

The domain of Hsp90 involved in binding C0818 was determined by constructing three truncation mutants: N-Hsp90, M-Hsp90 and C-Hsp90, corresponding to its ATP-binding domain, its co-chaperone binding domain and its dimerization domain. The fluorescence intensity of C-Hsp90, but not N-Hsp90 or M-Hsp90, was the most obviously quenched with increasing concentrations of C0818, indicating that C0818 may interact with the C-terminal domain (Fig. 5). The dissociation constant K_D values are listed in Table 5.

3.2. C0818 inhibits the ATPase activity of Hsp90

To characterize the inhibition of Hsp90 by C0818 binding, a colorimetric assay for inorganic phosphate was used to measure the inhibitory effect of C0818 on the ATPase activity of Hsp90. This assay is based on the formation of a phosphomolybdate complex and a subsequent reaction with malachite green. When the concentration of ATP was 1 mmol/L, the IC_{50} values of C0818 and GA were 120.74 and 0.41 $\mu\text{mol/L}$, respectively. Fig. 6 demonstrates the inhibition of Hsp90 ATPase activity by C0818. GA is a potent antiproliferative

agent but is not an ideal clinical agent due to its marked hepatotoxicity and narrow therapeutic window⁹. C0818, a small-molecule inhibitor, may have potential as a therapeutic agent with improved pharmacological properties compared to GA.

4. Discussion

Quenching of the fluorescence from a macromolecule can be classified as static quenching or dynamic quenching. In static quenching, the stability of new complexes of quenching agent and fluorescent material results in the decrease of the quenching constant of fluorescence. In dynamic quenching, the excited state molecules of quenching agent and fluorescent material collide with each other, resulting in energy transfer²⁰.

Our data suggest that C0818 is an Hsp90 inhibitor. Compared with the known inhibitor GA, C0818 has a novel scaffold unrelated to that of any other known Hsp90 inhibitor. Spectroscopic methods were used to study the interaction between C0818 and full-length Hsp90, N-Hsp90, M-Hsp90 and C-Hsp90. From the binding energy and dissociation constants, we demonstrated that C0818 is an inhibitor of Hsp90 and that it binds to the C-terminal dimerization domain of Hsp90. The quenching effect of C0818 on Hsp90 intrinsic fluorescence can thus be classified as static quenching. The thermodynamic parameters and the synchronous fluorescence suggest that electrostatic interactions predominate in stabilizing the C0818–Hsp90 complex.

C0818 inhibits the ATPase activity of Hsp90, so the binding of C0818 inhibits the catalysis of ATP hydrolysis. The binding of Hsp90 pockets arrests the catalytic cycle of Hsp90 in the ADP-bound conformation. The affinity-based screen showed that C0818 binds to Hsp90, therefore confirming the interaction between Hsp90 and C0818. In the assay measuring ATPase activity of Hsp90, C0818 demonstrated dose-dependent inhibition of the ATPase activity of Hsp90. As expected, the positive control GA also showed dose-dependent inhibition in this system.

Acknowledgments

The authors gratefully acknowledge the National Science and Technology Foundation of China for Key Projects of “Major New Drugs Innovation and Development” (2012ZX09103-101-028), Fujian Provincial Health and Family Planning Commission of China (2015-1-72), the Projects of Industry-Academy Cooperation for Science and Technology of Fujian Province, Chian (2016Y4005) for this project.

References

1. Wegele H, Müller L, Buchner J. Hsp70 and Hsp90-a relay team for protein folding. In: Adrian RH, Helmreich E, Holzer H, Jung R, Kramer K, Krayer O, editors. *Reviews of Physiology, Biochemistry and Pharmacology*. Berlin Heidelberg: Springer; 2004. p. 1–44.
2. Richter K, Hendershot LM, Freeman BC. The cellular world according to Hsp90. *Nat Struct Mol Biol* 2007;**14**:90–4.
3. Noguchi M, Yu D, Hirayama R, Ninomiya Y, Sekine E, Kubota N, et al. Inhibition of homologous recombination repair in irradiated tumor cells pretreated with Hsp90 inhibitor 17-allylamino-17-demethoxygeldanamycin. *Biochem Biophys Res Commun* 2006;**351**:658–63.
4. Soga S, Neckers LM, Schulte TW, Shiotsu Y, Akasaka K, Narumi H, et al. KF25706, a novel oxime derivative of radicicol, exhibits *in vivo* antitumor activity via selective depletion of Hsp90 binding signaling molecules. *Cancer Res* 1999;**59**:2931–8.
5. Harashima K, Akimoto T, Nonaka T, Tsuzuki K, Mitsuhashi N, Nakano T. Heat shock protein 90 (Hsp90) chaperone complex inhibitor, radicicol potentiated radiation-induced cell killing in a hormone-sensitive prostate cancer cell line through degradation of the androgen receptor. *Int J Radiat Biol* 2005;**81**:63–76.
6. Neckers L. Heat shock protein 90: the cancer chaperone. *J Biosci* 2007;**32**:517–30.
7. Taipale M, Jarosz DF, Lindquist S. HSP90 at the hub of protein homeostasis: emerging mechanistic insights. *Nat Rev Mol Cell Biol* 2010;**11**:515–28.
8. Schulte TW, Neckers LM. The benzoquinone ansamycin 17-allylamino-17-demethoxygeldanamycin binds to HSP90 and shares important biologic activities with geldanamycin. *Cancer Chemother Pharmacol* 1998;**42**:273–9.
9. Supko JG, Hickman RL, Grever MR, Malspeis L. Preclinical pharmacologic evaluation of geldanamycin as an antitumor agent. *Cancer Chemother Pharmacol* 1995;**36**:305–15.
10. Wu LX, Xu JH, Huang XW, Zhang KZ, Wen CX, Chen YZ. Down-regulation of P210^{bcr/abl} by curcumin involves disrupting the molecular chaperone functions of Hsp90. *Acta Pharmacol Sin* 2006;**27**:694–9.
11. Chen C, Lui Y, Chen YZ, Xu JH. C086, a novel analog of curcumin, induces growth inhibition and down-regulation of NF- κ B in colon cancer cells and xenograft tumors. *Cancer Biol Ther* 2011;**12**:797–807.
12. Wu LX, Yu J, Chen RJ, Liu Y, Lou LG, Wu Y, et al. Dual inhibition of Bcr-Abl and Hsp90 by C086 potently inhibits the proliferation of imatinib-resistant CML Cells. *Clin Cancer Res* 2015;**21**:833–43.
13. Chen JJ, Guo QJ, He XM, Yang SX, Chen C, Zhang LR. Study on a screening model for inhibitor of Hsp90 ATPase activity. *J Xiamen Univ Nat Sci* 2010;**49**:711–6.
14. Gao PZ, Wu H, Guo J, Xu YM. Study on the interaction between breviscapin and bovine serum albumin by fluorescence spectrometry. *Chin J Mod Appl Pharm* 2012;**29**:106–9.
15. Zhang GJ, Keita B, Brochon JC, de Oliveira P, Nadjo L, Craescu CT, et al. Molecular interaction and energy transfer between human serum albumin and polyoxometalates. *J Phys Chem B* 2007;**111**:1809–14.
16. Chen GZ, Huang XZ, Xu JG, Wang ZB, Zheng ZX. *Principles of fluorescent spectroscopy*. Beijing: Science Press; 1990.
17. Pastukhov AV, Levchenko LA, Sadkov AP. Spectroscopic study on binding of rutin to human serum albumin. *J Mol Struct* 2006;**842**:60–6.
18. Yan CN, Tong JQ, Xiong D, Liu Y, Pan ZT. Studies on the binding reaction features between pefloxacin and bovine serum albumin by fluorescence spectrophotometry. *Chin J Analyt Chem* 2006;**34**:796–800.
19. Ross PD, Subramanians S. Thermodynamics of protein association reactions: forces contributing to stability. *Biochemistry* 1981;**20**:3096–102.
20. Fleming K. Introduction to fluorescence theory and methods. *Techniq Biophys* 2005;**8**:1–11.